Inorganic Chemistry
Article
Cite This: Inorg. Chem. 2018, 57, 14834−14842
pubs.acs.org/IC

Preparation and Properties of Chlorosulfuryl Chloroformate, ClC(O)OSO$_2$Cl

Rosana M. Romano,*[,†] Angélica Moreno Betancourt,[†] Carlos O. Della Védova,[†] Xiaoqing Zeng,[‡] Helmut Beckers,[§] Helge Willner,[∥] Jan Schwabedissen,[⊥] and Norbert W. Mitzel*[,⊥]

[†]CEQUINOR (UNLP, CCT-CONICET La Plata), Departamento de Química, Facultad de Ciencias Exactas, Universidad Nacional de La Plata. Boulevard 120, N° 1465, La Plata CP1900, Argentina

[‡]College of Chemistry, Chemical Engineering and Materials Science, Soochow University, Suzhou 215123, Jiangsu, China

[§]Institut für Chemie und Biochemie, Anorganische Chemie, FU Berlin, Fabeckstraße 34/36, Berlin 14195, Germany

[∥]FB C, Anorganische Chemie, Bergische Universität Wuppertal, Gaußstraße 20, Wuppertal 42119, Germany

[⊥]Fakultät für Chemie, Lehrstuhl für Anorganische Chemie und Strukturchemie, Universität Bielefeld, Universitätsstraße 25, Bielefeld 33615, Germany

Supporting Information

ABSTRACT: The novel chlorosulfuryl chloroformate, ClC(O)OSO$_2$Cl, was prepared by the reaction of CCl_4 and SO_3. Alternatively, the compound was obtained from the direct insertion reaction of SO_3 to $Cl_2C{=}O$. The latter reaction constitutes also a confirmation of the proposed mechanism for the former one. Density functional theory and MP2 theoretical approximations predict the existence of two conformers, syn−gauche and syn−anti, depending on the value adopted by the dihedral angles ϕ(Cl−C−O−S) and ϕ(C−O−S−Cl). The structure of the syn−gauche conformer was determined by gas-phase electron diffraction (GED). The existence of the syn−anti conformer can be neither confirmed nor excluded by the GED experiment. Vibrational spectra (vapor-phase and argon-matrix Fourier transform infrared and liquid Fourier transform Raman) were interpreted by an equilibrium mixture between both conformers.

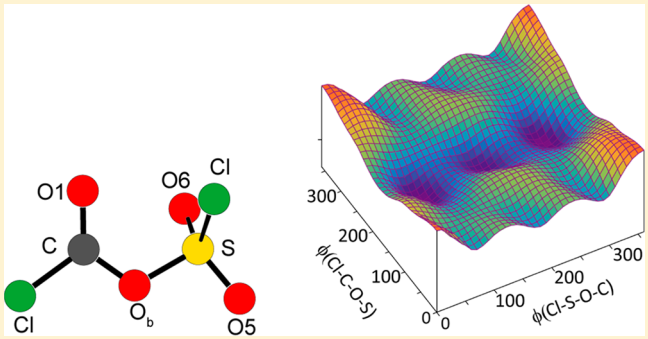

INTRODUCTION

Because of their high reactivity, derivatives of sulfuric acid, like fluoro- or chlorosulfonic acid, sulfuryl chloride, or disulfuric acid and many more play important roles in synthetic and industrial chemistry. In spite of the fact that they have been widely used for more than a century, many aspects of their spectroscopic and structural chemistry are still to be uncovered. Very recently, we reported the extreme polymorphism of disulfuryl dichloride, ClSO$_2$OSO$_2$Cl, in its crystalline form of appearance and its conformational behavior in the gas phase, unraveled by vibrational spectroscopy and gas-phase electron diffraction (GED).[1]

The reaction between sulfur trioxide and carbon tetrachloride to afford this disulfuryl dichloride was first reported by Schützenberger in 1869[2] and interpreted by eq 1:

$$CCl_4 + 2SO_3 \rightarrow ClSO_2OSO_2Cl + Cl_2C{=}O \quad (1)$$

Since that time, this reaction has been extensively used for the preparation of either disulfuryl dichloride, ClSO$_2$OSO$_2$Cl, or phosgene, $Cl_2C{=}O$ (see, for example, ref 3). In this work, we reinvestigated the chemical reaction between SO_3 and CCl_4 using different proportions of the reactants. When the reaction was performed in excess of SO_3, a third product was formed. On the basis of the evidence of IR spectroscopy, the formation of a hitherto unknown compound, chlorosulfuryl chloroformate [ClC(O)OSO$_2$Cl], was proposed (eq 2).

$$CCl_4 + 3SO_3 \rightarrow ClSO_2OSO_2Cl + ClC(O)OSO_2Cl \quad (2)$$

The following two-step mechanism interprets the reaction:

$$CCl_4 + 2SO_3 \rightarrow ClSO_2OSO_2Cl + Cl_2C{=}O \quad (1)$$

$$Cl_2C{=}O + SO_3 \rightarrow ClC(O)OSO_2Cl \quad (3)$$

The use of a closed system favored the second step of this mechanism (eq 3) because the generated phosgene could not escape from the reaction mixture as in an open system. In order to prove the proposed mechanism, the reaction between phosgene and sulfur trioxide was investigated. ClC(O)OSO$_2$Cl was obtained as the only product in very high yield (>90%).

The compound was characterized by vibrational spectroscopy [vapor-phase Fourier transform infrared (FTIR), liquid

Received: September 11, 2018
Published: November 16, 2018

DOI: 10.1021/acs.inorgchem.8b02581
Inorg. Chem. 2018, 57, 14834−14842

FT-Raman, and argon-matrix FTIR spectra]. Its physical properties (density, melting point, and boiling point) were determined. The structure was determined by GED experiments. The conformational preferences are in agreement with the results computed with density functional theory (DFT) and MP2 theoretical methods.

EXPERIMENTAL METHODS

Synthesis. $ClC(O)OSO_2Cl$ was prepared by two alternative methods. In the La Plata laboratories, CCl_4 was condensed together with fresh prepared SO_3 in a Carius tube provided with a Young valve under vacuum conditions. SO_3 was prepared by heating a reactor containing $Na_2S_2O_8$ or $K_2S_2O_8$ at 270 °C to obtain either $Na_2S_2O_7$ or $K_2S_2O_7$. These salts were subsequently heated with a Bunsen burner to generate SO_3, which was collected in a U trap kept at −196 °C in its trimeric form. The trimer was subsequently transformed into its monomer by heating at approximately 120 °C under vacuum. Mixtures of SO_3 and CCl_4 in different molar proportions (2:1, 3:1, and 4:1) were stirred at 80 °C for 2 h. The product was isolated and purified by repeated trap-to-trap distillation in vacuum conditions, with traps maintained at −50, −110, and −196 °C. Pure $ClC(O)OSO_2Cl$ was retained in the −50 °C trap. The best yield (~50%) was obtained in the reaction of a 3:1 SO_3/CCl_4 mixture.

In the Wuppertal laboratories, $Cl_2C{=}O$ and SO_3 were mixed in different proportions in a cell with a Young valve, specially designed to follow the course of the reaction by Raman spectroscopy. The reaction mixtures were maintained at different temperatures, ranging from 20 to 50 °C, and also for different reaction times, from 1 min to 3 days. No reaction was observed in these experiments; i.e., the mixtures were completely stable under these conditions. In a second series of experiments, the reactants in the condensed phases were sealed in glass tubes and heated up to 80 °C (the vapor pressure of phosgene at 80 °C is ~9 bar). Different proportions and reaction times were tested, and the course of the reactions in the sealed tubes was followed using Raman spectroscopy. The best yield (higher than 90%) was obtained after 5 h of reaction at 80 °C, starting with a 2:1 $Cl_2C{=}O/SO_3$ mixture. $ClC(O)OSO_2Cl$ was obtained as the only product, by means of eq 3. The remaining sulfur trioxide was eliminated using KCl, which with SO_3 forms a nonvolatile salt, KSO_3Cl. The excess of phosgene was removed by trap-to-trap distillation in vacuum.

Physical Properties. $ClC(O)OSO_2Cl$ was a colorless liquid at ambient temperatures. The boiling point, measured at 33.9 mbar, was 42.0 °C. The white solid melted at −12.2 °C to a transparent liquid. The density of the liquid at room temperature was found to be 1.61 g/mL.

Vibrational Spectroscopy. FTIR spectra were recorded in La Plata in a Thermo Nexus Nicolet FTIR instrument equipped with a cryogenic MCTB detector for the ranges 4000−400 cm^{-1} in a 10 cm gas cell with silicon windows. In Wuppertal, a Bruker Vector 25 spectrometer was used. The Raman spectra of liquid samples were taken with a Bruker Equinox 55 FRA 106/S FT-Raman spectrometer equipped with a 1064 nm Nd:YAG laser.

Matrix Isolation Experiment. A few milligrams of $ClC(O)OSO_2Cl$ were condensed into a U trap connected to an inlet nozzle of the matrix equipment, consisting of a quartz tube of an internal diameter of 4 mm and an outlet opening of 1 mm diameter. An argon flux of 2 mmol/h was directed to the sample held at −61 °C, and the mixture was deposited on the cold matrix support (15 K, rhodium-plated copper block) in a high vacuum. Details of the matrix apparatus were given elsewhere.[4] Temperature-dependent experiments were carried out by passing mixtures of the gaseous sample and argon through a quartz nozzle (1 mm i.d.), heated over a length of ~10 mm with a platinum wire (0.25 mm o.d.) prior to deposition on the matrix support. The nozzle was held at 158, 250, or 350 °C. Photolysis experiments were performed with a high-pressure mercury lamp (TQ150, Heraeus) using a water-cooled quartz lens optic.

UV−Visible Spectra. The gas-phase UV−visible spectra were recorded in a gas cell at different pressures. In the range between 190 and 800 nm, $ClC(O)OSO_2Cl$ does not present any electronic absorption, at least with appreciable intensity.

GED Experiment. The electron diffraction patterns were recorded using the heavily improved Balzers Eldigraph KD-G2 gas-phase electron diffractometer at Bielefeld University. Experimental details are listed in Table 1, and instrumental details are reported elsewhere.[5]

Table 1. Details of the GED Experiment for $ClC(O)OSO_2Cl$

	detector distance	
	short	long
nozzle-to-plate distance, mm	250.0	500.0
accelerating voltage, kV	60	60
fast electron current, μA	1.50	1.49
electron wavelength,[a] Å	0.048337	0.048641
nozzle temperature, K	293	292
sample pressure,[b] mbar	3×10^{-7}	8.7×10^{-7}
residual gas pressure,[c] mbar	6.8×10^{-8}	8.6×10^{-8}
exposure time, s	7	7
used s range, $Å^{-1}$	8.0−31.5	2.1−14.5
number of inflection points[d]	5	4
R_f factor	7.441	2.822

[a]Determined from CCl_4 diffraction patterns measured in the same experiment. [b]During the measurement. [c]Between measurements. [d]Number of inflection points on the background lines.

The electron diffraction patterns, three for each, long and short, nozzle-to-plate distance, were measured on Fuji BAS-IP MP 2025 imaging plates, which were scanned by using a calibrated Fuji BAS.1800II scanner. The intensity curves (Figure 1) were obtained by

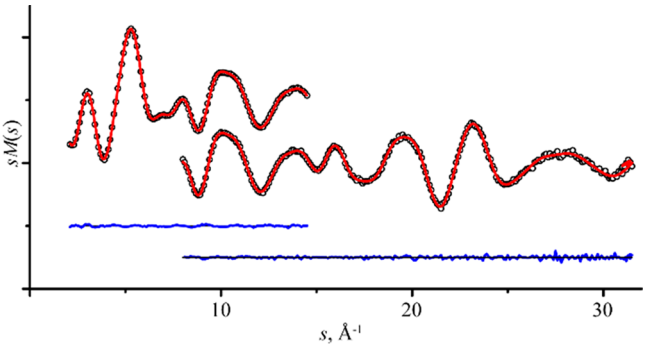

Figure 1. Experimental (O) and model (—) molecular intensity curves of $ClC(O)OSO_2Cl$ for long (upper trace) and short (lower trace) nozzle-to-detector distance and the difference curves, respectively.

applying the method described earlier.[6] The sector function and electron wavelength were refined[7] using carbon tetrachloride diffraction patterns, recorded in the same experiment as the substance under investigation.

Gas-Phase Structure Analysis. Structural analysis was performed using the *UNEX* program.[8] All refinements were performed using two averaged intensity curves simultaneously (Figure 1), one from the short and another from the long nozzle-to-plate distance, which were obtained by averaging independent intensity curves measured in several experiments.

The refinement was performed by employing a two-conformer model composed of the syn−gauche and syn−anti conformers, as suggested by quantum-chemical calculations (see below). In the course of the refinement, the gas-phase composition of $ClC(O)OSO_2Cl$ was varied according to the least-squares refinement, resulting in a low amount of the syn−anti conformer. Hence, a refinement only considering the syn−gauche conformer was

DOI: 10.1021/acs.inorgchem.8b02581
Inorg. Chem. 2018, 57, 14834−14842

performed, which resulted in a satisfactory accordance to the experiment. The starting values for the structural parameters as well as the fixed differences between the values of the parameters refined in one group were taken from the MP2/cc-pVTZ calculations. In order to calculate the starting values for amplitudes of vibrations and curvilinear corrections to the equilibrium structure used in the GED refinements, analytical quadratic and numerical cubic force fields were calculated for all conformers employing the MP2/cc-pVTZ approximation. The mean-square amplitudes and vibrational corrections to the equilibrium structure were calculated using the *SHRINK* program.[9]

Quantum Chemistry. The potential energy scan was performed using the *Firefly* program[10] with the O3LYP/cc-pvtz level of theory (which earlier proved to provide a good description of related molecules like $ClSO_2OSO_2Cl$[1]). Optimizations of the conformers were carried out using the *Gaussian 09*, version D01.[11] Calculations of the vibrational properties were carried out at potential-energy-minimum geometries for which no imaginary vibrational frequency was found. Natural bond orbital (NBO) analysis was performed with the *NBO6* program[12] incorporated in *Gaussian 09*. The atoms-in-molecules (AIM) properties were calculated using the program *AIMALL*.[13]

RESULTS AND DISCUSSION

Quantum-Chemical Investigation. For determination of the possible conformers existing in the gas phase, a two-dimensional potential energy surface was calculated on the O3LYP/cc-pvtz[14] level of theory by rotating the chloroformyl group around the central C−O bond independently from the rotation of the chlorosulfuryl group around the central S−O bond (Figure 2). From the potential energy surface depicted in

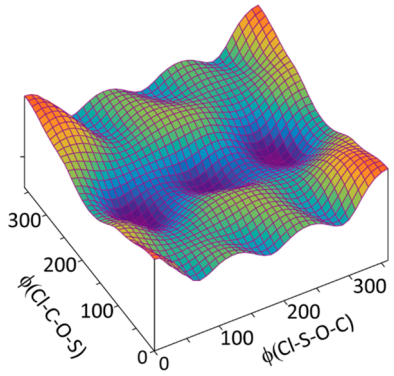

Figure 2. Potential energy surface calculated on the O3LYP/cc-pvtz level of theory by independently rotating the two dihedral angles ϕ(Cl−C−O−S) and ϕ(Cl−S−O−C) of $ClC(O)OSO_2Cl$.

Figure 2, it is recognizable that the dihedral angle ϕ(Cl−C−O−S) can adopt two different values, 180 and 0°, corresponding to the syn and anti conformations of the O_b−S bond relative to the C═O bond. On the other hand, the S−Cl bond can adopt two different orientations relative to the carbonyl group, a gauche conformation with a dihedral angle ϕ(Cl−S−O−C) of about 60° and a multiplicity of 2 and an anti conformation with a dihedral angle ϕ(Cl−C−O−C) of 180°.

The four structures observed as energy minima in the potential energy surface of Figure 2, syn−gauche, syn−anti, anti−gauche, and anti−anti, were subsequently fully optimized and characterized as minima for which no imaginary frequencies occur using different levels of theory and basis set combinations. The conformers with anti orientation of the O−S bond with respect to the C═O bond are approximately 17−18 kJ/mol higher in energy than the syn conformer, as calculated with the B3P86/6-31+G(d) level of approximation, and will not be considered in the further discussion. The molecular models of the syn conformers are presented in Figure 3. Some selected geometry parameters of the optimized

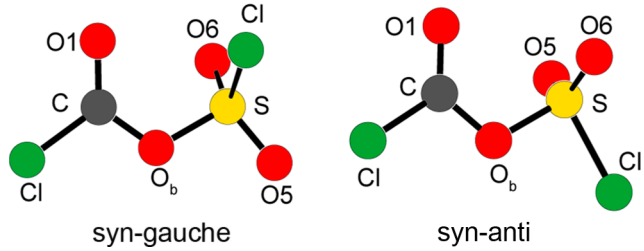

Figure 3. Molecular models of the syn−gauche and syn−anti conformers of $ClC(O)OSO_2Cl$ calculated at the B3LYP/cc-pvtz level of theory.

syn−gauche and syn−anti conformers, with C_1 and C_s symmetry, respectively, are listed in Table 2. The abundance of the syn−anti conformer decreases along the series B3LYP,[15] B2PLYP,[16] and MP2[17] from 22% to 15%.

Previously investigated chloroformates of the type ClC(O)-OX also favor syn conformations, with the C═O bond being synperiplanar to the O−X bond. For example, the trifluoromethyl chloroformate $ClC(O)OCF_3$[18] shows stabilization of 16−20 kJ/mol for the syn conformer, depending on the method used. In the related trichloromethyl chloroformate ("diphosgene") $ClC(O)OCCl_3$,[19] the syn conformer is lower in energy by 20 kJ/mol (B3LYP) to 28 kJ/mol (MP2) than the anti conformer.

On the other hand, other carbonyl sulfonates behave differently compared to the substance under investigation regarding the orientation of the C−O bond with respect to the S−X bond. The trifluoromethanesulfonates $ClC(O)-OSO_2CF_3$[20,21] and $FC(O)OSO_2CF_3$[22] show that the gauche conformer (the C−S bond is gauche with respect to the C−O bond) is not the global minimum on the energy surface. In both cases, an anti conformation, analogous to the one depicted in Figure 3, is the conformer of lower energy, and a gauche conformer is by approximately 4 kJ/mol higher in energy. This is different from that for $ClC(O)OSO_2Cl$, with the gauche conformer being lowest in energy.

Table 2 shows no variation of the C−Cl bond between both conformers, whereas the S−Cl bond is longer by 0.002 Å in the syn−gauche conformer. The most sensitive parameter regarding the conformation of the molecule is the central S−O_b bond (the subscript b means bridging O), which is by about 0.01 Å shorter in the syn−gauche conformer. This is consistent with the less pronounced elongation of the C−O_b bond in the syn−gauche conformer. The central angle ∠(S−O−C) varies by 5° among the conformers, measuring about 120° in the syn−gauche conformer and being significantly lower in the syn−anti conformer. Among the different DFT[23] and ab initio methods listed in Table 2, the bonds containing one or two elements of the third row of the periodic table shorten with increasing consideration of the electron correlation along the series B3LYP, B2PLYP, and MP2. Furthermore, the C−O_b bond elongates in the same order. The characteristic dihedral angle of the syn−gauche conformer ϕ(Cl−S−O−C) is predicted to be about 69° by all methods.

DOI: 10.1021/acs.inorgchem.8b02581
Inorg. Chem. 2018, 57, 14834−14842

Table 2. Selected Structure Parameters of the Syn−Gauche and Syn−Anti Conformers of $ClC(O)OSO_2Cl$

theoretical method	conformer	geometrical parameter[a] r(S−Cl)	r(C−Cl)	r(S−O_b)	r(C−O_b)	∠(S−O−C)	ϕ(Cl−S−O−C)	% syn−anti[b]
MP2/cc-pvtz	syn−gauche	2.019	1.730	1.655	1.379	118.9	68.4	
	syn−anti	2.016	1.730	1.669	1.375	114.5	180.0	15.4
B2PLYP/cc-pvtz	syn−gauche	2.037	1.743	1.665	1.375	120.1	68.7	
	syn−anti	2.035	1.743	1.678	1.372	115.9	180.0	19.6
B3LYP/cc-pvtz	syn−gauche	2.052	1.752	1.674	1.372	121.0	69.0	
	syn−anti	2.050	1.752	1.686	1.369	116.8	180.0	22.2

[a]Distances r are in angstroms and angles and dihedral angles in degrees. [b]Abundancy is calculated on the basis of $\Delta G°$ values.

Gas-Phase Structure. The gas-phase structure of $ClC(O)OSO_2Cl$ was determined by means of electron diffraction using a two-conformer model. In this refinement, the composition in the gas phase was refined as a free parameter. In the further progress of the refinement, the percentage of the syn−anti conformer became so low that a single-conformer model was tested, resulting in a reasonably good agreement with the experimental diffraction data. In total, five groups of bonded distances, six angles, three dihedrals, and nine groups of amplitudes of vibration were refined. Figure 4 shows the radial distribution curve along with the difference curve.

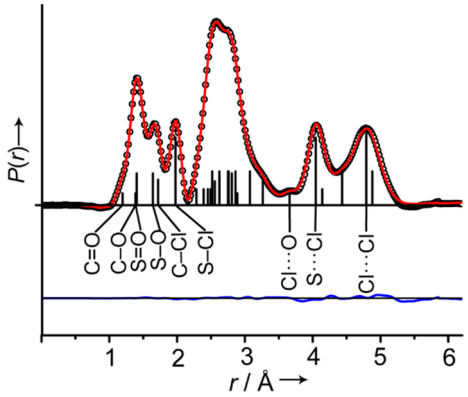

Figure 4. Experimental (○) and model (—) radial distribution functions of $ClC(O)OSO_2Cl$. The difference curve is below. Vertical bars indicate interatomic distances; select distances are labeled.

The GED experiment cannot confirm the existence of a syn−anti conformer. Significant contributions of the syn−anti conformer to the radial distribution curve are expected at distances above 3.5 Å, i.e., the interatomic Cl−Cl distance of this conformer. Although the difference curve in this region shows a slight discrepancy between the model and experiment, only the contribution of the Cl···O term for the syn−gauche conformer is found at about 3.6 Å. Structural parameters of the refined gas-phase structure are listed in Table 3 along with the structures of related molecules.

Previously determined gas-phase structures show some similarities to as well as differences from the one here examined. A shorter C−Cl bond is found in $ClC(O)OSO_2Cl$ [1.711(2) Å] compared to analogous distances in $ClC(O)OCH_2CCl_3$[24] [1.744(2) Å] and in $ClC(O)OCF_3$[18] [1.726(4) Å]. On the other hand, the carbonyl C═O bond is rather long [1.192(3) Å] but also lies within the error range of the bond lengths of related molecules. The central angle at the oxygen atom (∠C−O−X) varies in the group of listed chloroformates between 110.6(23)° and 117.6(6)°, and the more electronegative the substituent, the wider the angle. The gas-phase structures of the trifluoromethyl[18] and methyl[25] chloroformates show an anti orientation regarding the C−O single bond, whereas the trichloroethyl derivative shows a dynamic behavior in the gas phase. When the structural parameters of the $ClSO_2$ fragments in previously examined samples are compared with the one investigated here, a shorter Cl−S bond is found at 1.967(2) Å. The central angle [113.9(6)°] is the same, within the range of errors, as that observed for the methylated compound $ClSO_2OCH_3$[26] [114.4(11)°] but by far more narrow than that in the analogous CF_3 species[27] [122.2(12)°]. The conformation of all three chlorosulfuryl species is gauche regarding the orientation of the O−C single bond relative to that of the S−Cl bond. In comparison to the recently investigated symmetric pyrosulfuryl dichloride,[1] a shorter bond of the sulfur atom to the bridging oxygen atom is observed for $ClSO_2OSO_2Cl$ and a longer S−Cl bond is found in the latter case. Furthermore, the gas-phase structure was as

Table 3. Experimental Geometrical Parameters of Several Chloroformate- or Chlorosulfuryl-Containing Molecules

parameter[a]	(rC−Cl)	r(C═O)	r(C−O_b)	r(S−O_b)	r(S−Cl)	∠(SOC)[b]	∠(ClCO)	∠(ClSO)	ϕ(ClSOC)	ref
$ClC(O)OSO_2Cl$, r_e	1.711(2)	1.192(3)	1.379(4)	1.635(2)	1.967(1)	113.9(6)	108.1(5)	104.1(5)	68.3(8)	this work
$ClC(O)OCH_2CCl_3$,r_e	1.744(2)	1.184(8)	1.327(9)			110.6(23)	108.9(14)		[c]	24
$ClC(O)OCF_3$, syn, r_α	1.726(4)	1.185(5)	1.371(6)			117.6(6)	107.7(1)		0.0 (C_s)[d]	18
$ClC(O)OCH_3$, MW	1.73(2)	1.19(2)	1.36(2)			115(2)	109(2)		0.0 (C_s)[e]	25
$ClSO_2OCF_3$, r_α				1.606(6)	1.999(3)	122.2(12)		97.3(19)	94(3)	27
$ClSO_2OCH_3$, r_a				1.562(4)	2.023(4)	114.4(11)		102.8(14)	74(4)	26
$ClS(O)_2OS(O)_2Cl$, r_g				1.626(1)	1.992(1)	127.2(2)			80.5(4)	27
SO_2Cl_2, r_g					2.012(4)			100.3(2)		28
$ClSO_2OSO_2Cl$, r_e				1.617(1)	1.985(1)	127.2(2)		98.7(3)	80.5(4)[f]	1

[a]Distances r are in angstroms and angles and dihedral angles in degrees. [b]In the cases of $ClC(O)OCH_2CCl_3$ and $ClC(O)OCF_3$, the central angle ∠(C−O−C) is given. [c]In this case, the refinement was performed using a dynamic model. Thus, no explicit ϕ(C−C−O−C) is given. [d]The dihedral angle ϕ(F−C−O−C) is given. [e]The dihedral angle ϕ(H−C−O−C) is given. [f]The dihedral angle ϕ(Cl−S−O−S) is reported.

DOI: 10.1021/acs.inorgchem.8b02581
Inorg. Chem. 2018, 57, 14834−14842

well determined by using a one-conformer model like in the current investigation, in spite of the fact that quantum-chemical calculations suggested a multiconformer composition.

An appropriate molecule to compare the entire structure with is $FC(O)OSO_2CF_3$.[22] As mentioned above, its gauche conformation for the C−O−S−C dihedral angle is less preferred. GED data revealed that the vapor consists of 33(8)% of the gauche conformer, while the anti conformer is exclusively present in the crystalline phase. Compared to the substance investigated here, the conformational preference is reversed, and in the case of $ClC(O)OSO_2Cl$, no other conformer is observed in the gas phase. Interestingly, the crystal structure of $ClC(O)OSO_2CF_3$[20] contains both anti and gauche conformers.

Quantum-Chemical Study of Conformational Preferences. To investigate the different kinds of stabilizing interactions for the syn−gauche and syn−anti conformers, different schemes were applied to both conformers. All calculations were performed at the B3LYP/aug-cc-pvtz level of theory. As a first step, NBO analysis[28] was performed. Table 4 lists the most significant interactions of high value or

Table 4. Most Important Donor → Acceptor Interactions (kJ/mol) Calculated for Both Conformers of $ClC(O)OSO_2Cl$ Using the NBO Algorithm

interaction (donor → acceptor)	syn−gauche	syn−anti
$lp(O_b) \rightarrow \pi^*(C{=}O)$	162	169
$lp(O_b) \rightarrow \sigma^*(S{-}Cl5)$	32	*a*
$lp(Cl5) \rightarrow \sigma^*(S{-}O_b)$	28	24
$lp(O6) \rightarrow \sigma^*(S{-}O_b)$	49	63
$lp(O6) \rightarrow \sigma^*(S{-}Cl5)$	50	40
$lp(O6) \rightarrow \sigma^*(S{-}O_b)$	127	111
$lp(O6) \rightarrow \sigma^*(S{-}Cl5)$	108	117
$lp(O7) \rightarrow \sigma^*(S{-}O_b)$	43	63
$lp(O7) \rightarrow \sigma^*(S{-}Cl5)$	47	40
$lp(O7) \rightarrow \sigma^*(S{-}O_b)$	108	111
$lp(O7) \rightarrow \sigma^*(S{-}Cl5)$	110	117
$\sigma(S{-}Cl5) \rightarrow \sigma^*(S{-}O_b)$	27	18
$\sigma(S{-}O_b) \rightarrow \sigma^*(S{-}Cl5)$	18	23
$\sigma(S{-}O7) \rightarrow \sigma^*(S{-}O_b)$	15	24

[a]This interaction is below the threshold (2 kJ/mol) of the NBO scheme and is thus not given here. The atom numbering is shown in Figure 3.

distinguishing the conformers most clearly. Both conformers have a high value for the conjugation effect of the lone pair of the bridging oxygen atom into the antibonding π^* orbital of the C=O bond. In this interaction, the conjugative effects within the carboxyl group are manifest. The most distinguishing interaction between both conformers is the electron density donation of the lone pair of the bridging oxygen atom into the antibonding σ^* orbital of the S−Cl bond. This interaction is unique in the syn−gauche conformer or, more precisely, lower than the threshold (2 kJ/mol) in the syn−anti conformer because the $-SO_2Cl$ group is rotated to prefer this interaction in the syn−gauche conformer. Because the preference of the gauche conformation, the stabilizing effect of the donation forming a lone pair of electrons belonging to the chlorine atom bonded to the sulfur atom into the antibonding σ^* orbital of the central $S{-}O_b$ bond increases by 4 kJ/mol. Interactions within the chlorosulfuryl group are approximately equal in both conformers. The donation involving the bonding and antibonding orbitals favor the syn−anti conformer by approximately 5 kJ/mol. Thus, on the basis of the NBO donor−acceptor formalism, no clear preference can be justified.

For further investigation of the different stabilizations in the two conformers, steric analysis[29] of the natural orbitals was performed. In this analysis, steric interactions destabilizing the molecule were calculated; selected interactions are listed in Table 5. The lone pairs of electrons of the central oxygen atom

Table 5. Selected Orbital Interactions in the NBO Analysis Scheme (kJ/mol) in the Two Conformers of $ClC(O)OSO_2Cl$

interacting orbitals	syn−gauche	syn−anti
$lp(O_b){-}\sigma(C{-}Cl)$	14	18
$lp(O_b){-}\sigma(C{=}O)$	59	61
$lp(O_b){-}\sigma(S{-}Cl)$	16	20
$lp(O6){-}\sigma(S{-}O_b)$	35	26
$lp(O7){-}\sigma(S{-}O_b)$	11	16
$lp(O8){-}\sigma(C{-}Cl)$	60	57
$lp(O8){-}\sigma(C{-}O)$	50	50

are interacting repulsively with the electrons of the C−Cl, C=O, and S−Cl bonds, resulting in destabilization of the syn−anti conformer by about 9 kJ/mol. However, in the interaction of the lone pair of a sulfuryl oxygen atom, the $S{-}O_b$ bond is destabilizing the syn−gauche conformer by the same magnitude.

As a third tool, the quantum theory of AIM[30] was applied to both conformers (Table 6). In this theory, molecular properties are based on the electron density ρ. In the C−Cl bond, both conformers are distinct in their electron density at the bond critical point (bcp) by 0.06 e/a_0^3. The Laplacian of electron density $\nabla^2(\rho)$ in the $S{-}O_b$ bond is more positive in the syn−gauche conformer, which means that the covalent

Table 6. Specific Values Taken from an Electron Density Calculation for Selected Bonds of Both Conformers of $ClC(O)OSO_2Cl$

	syn−gauche	syn−anti
	C−Cl	
ρ, e/a_0^3	2.039×10^{-1}	2.639×10^{-1}
$\nabla^2(\rho)$, e/a_0^5	-2.698×10^{-1}	-2.703×10^{-1}
bond path length, Å	1.752	1.751
bcp−C, Å	0.785	0.785
bcp−Cl, Å	0.967	0.967
ε	1.049×10^{-1}	1.031×10^{-1}
	$S{-}O_b$	
ρ, e/a_0^3	2.073×10^{-1}	2.060×10^{-1}
$\nabla^2(\rho)$, e/a_0^5	-3.794×10^{-1}	-4.272×10^{-1}
bond path length, Å	1.677	1.688
bcp−S, Å	0.685	0.700
bcp−O_b, Å	0.992	0.988
ε	7.585×10^{-2}	2.508×10^{-2}
	S−Cl	
ρ, e/a_0^3	1.553×10^{-1}	1.567×10^{-1}
$\nabla^2(\rho)$, e/a_0^5	-1.141×10^{-1}	-1.217×10^{-1}
bond path length, Å	2.051	2.049
bcp−S, Å	0.992	0.992
bcp−Cl, Å	1.059	1.057
ε	4.121×10^{-2}	2.516×10^{-2}

DOI: 10.1021/acs.inorgchem.8b02581
Inorg. Chem. 2018, 57, 14834−14842

character is reduced compared to the respective one of the syn−anti conformer. Furthermore, the bond ellipticity ε, which measures the anisotropy of the bond regarding the direction perpendicular to the bond path, is about 3 times larger in the syn−gauche conformer. The same issue occurs in the S−Cl bond, where the bond ellipticity is twice as large as that in the syn−gauche conformer. All of these effects stabilize the syn−gauche form.

Vibrational analysis. The vapor-phase FTIR and FT-Raman spectra of liquid $ClC(O)OSO_2Cl$ recorded for samples prepared by both synthetic methods described previously are identical, indicating the high purity of the samples. These spectra (Figure 5) were analyzed together with the FTIR

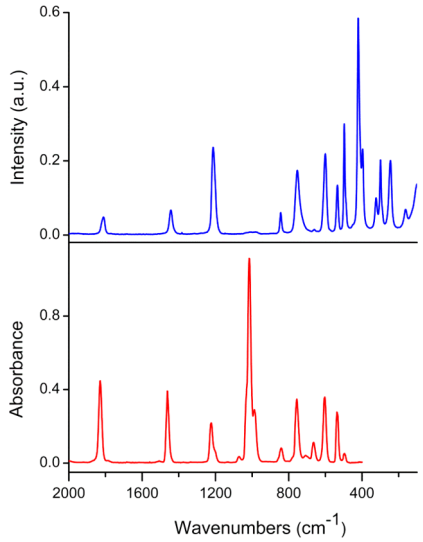

Figure 5. Vapor-phase FTIR (bottom, red trace; resolution = 2 cm^{-1}; pressure = 2 mbar; optical path = 10 cm) and FT-Raman (top, blue trace; liquid at ambient temperature; excitation at 1064 nm; 150 mW) spectra of $ClC(O)OSO_2Cl$.

spectrum of the compound isolated in an argon matrix in a 1:1000 proportion, the prediction of quantum-chemical calculations, and a comparison with the spectra of related molecules (e.g., refs 1, 18−22, 24, 25, and 31). Selected experimental wavenumbers of $ClC(O)OSO_2Cl$ for the vapor-phase FTIR, argon-matrix FTIR, and liquid Raman are listed in Table 7. The theoretical wavenumbers for both conformers calculated with the B3P86/6-31+G(d) and MP2/Aug-CC-pVTZ approximations are also included in Table 7.

As can be observed in Table 7, the vibrational spectra are consistent with an equilibrium between two conformers. Either in the vapor-phase FTIR spectrum or in the Raman spectrum of the liquid, the bands assigned to the second conformer appear in most cases as shoulders of the bands of the most stable form because of the small differences in the wavenumbers. However, in the FTIR spectrum of $ClC(O)OSO_2Cl$ isolated in the argon matrix, the absorptions assigned to the syn−anti conformer are clearly distinguished from the bands of the syn−gauche conformer because of the sharpening of the absorptions due to the elimination of intermolecular interactions and rotational effects in the matrix. Figure 6 presents selected regions of the FTIR spectrum of the matrix.

The C=O stretching wavenumber is a sensor of the nature of its substituents.[31] Its wavenumber is a function of the sum of the group electronegativities attached to it. For a series $ClC(O)OX$ with X = CF_3, SO_2Cl, SO_2CF_3, CCl_3, CH_3, and C_2H_5 with ν(C=O) = 1837 cm^{-1},[18] 1831/1826 cm^{-1} (syn−gauche/syn−anti conformer), 1829 cm^{-1} (syn−anti conformer),[20] 1823 cm^{-1},[19] 1801 cm^{-1},[25] and 1793 cm^{-1},[32,33] respectively, this trend behaves as predicted by Kagarise.[31] Moreover, this formalism predicts also the very similar C=O wavenumbers expected for the species $ClC(O)OSO_2Cl$ and $ClC(O)OSO_2CF_3$. In the title molecule, very small differences originating from different mesomeric contributions in the two syn−gauche and syn−anti conformations also complete this approximation.

The vibrational stretching modes assigned to the SO_2 group, $\nu_{as}(SO_2)$ and $\nu_s(SO_2)$, present values that are wholly consistent with the previously reported ones for molecules with the $-OSO_2Cl$ moiety.[1,34] Figure 6 shows two pairs of absorptions in the FTIR argon-matrix spectrum between 1460 and 1450 cm^{-1}, attributed to the $\nu_{as}(SO_2)$ of the syn−gauche (1458.5−1457.2 cm^{-1}) and syn−anti (1455.8−1454.0 cm^{-1}) conformers in two different matrix sites.

The most intense feature of the IR spectra of $ClC(O)OSO_2Cl$ corresponds to the stretching vibration of the C−O single bond. Three overlapped bands are observed in the gas-phase FTIR spectrum (Figure 5), which are fully resolved in the IR matrix-isolation spectrum (Figure 6). Besides ν(C−O) of the syn−anti (1034 cm^{-1}) and syn−gauche (1016 cm^{-1}) conformers, a combination band at 987 cm^{-1} [$\delta(SO_2) + \delta$(Cl−C=O)], enhanced by the Fermi resonance, is observed in the gas-phase FTIR spectrum. The positions of the ν(C−O) fundamentals completely agree with those observed for $ClC(O)OSO_2CF_3$, 1042 cm^{-1} (syn−anti conformer) and 1016 cm^{-1} (syn−gauche conformer).[20] The ν(S−O) fundamental is also sensitive to the conformation adopted by the molecule, as shown in Figure 6 and Table 7. Red shifts of about 20 cm^{-1} in the ν(C=O) and $\nu_{as}(SO_2)$ fundamentals in the Raman spectrum of the liquid compared with the IR spectrum of the vapor phase denote some association and the contact between the molecules in the liquid phase.

Pyrolysis and Photolysis of Matrix-Isolated $ClC(O)OSO_2Cl$. $ClC(O)OSO_2Cl$ is stable to pyrolysis up to 350 °C. The title compound is also stable under UV−visible photolysis in matrix conditions, in accordance with the absence of absorption bands in the UV−visible spectrum. Only extremely low amounts of SO_3, $Cl_2C=O$, and Cl_2SO_2 were produced upon photolysis. These traces were recognized by their absorptions at 1385 cm^{-1} (SO_3),[35] 1816/1814/837/836 cm^{-1} ($Cl_2C=O$),[36] and 1448/1427 and 1202 cm^{-1} (Cl_2SO_2; the band at 590 cm^{-1} is not visible because it overlaps with one of the compounds).[37] Then, two mechanisms can be proposed (eqs 4 and 5).

$$ClC(O)OSO_2Cl \rightarrow Cl_2C{=}O + SO_3 \quad (4)$$

$$ClC(O)OSO_2Cl \rightarrow Cl_2SO_2 + CO_2 \quad (5)$$

Reactions of $ClC(O)OSO_2Cl$. $ClC(O)OSO_2Cl$ reacts violently with water, resulting in phosgene (eq 6).

$$ClC(O)OSO_2Cl + H_2O \rightarrow Cl_2C{=}O + H_2SO_4 \quad (6)$$

The reaction with TlF gives $ClC(O)OSO_2F$ (eq 7), which subsequently decomposes into ClC(O)F and the salt $TlSO_3F$ (eq 8). This decomposition is favored when an excess of TlF is used.

DOI: 10.1021/acs.inorgchem.8b02581
Inorg. Chem. 2018, 57, 14834−14842

Table 7. Selected Experimental (Vapor-Phase FTIR, Argon-Matrix IR, and Liquid Raman) Wavenumbers (cm^{-1}) of $ClC(O)OSO_2Cl$, Calculated [B3P86/6-31+G(d) and MP2/Aug-CC-pVTZ] Wavenumbers for the Syn−Gauche and Syn−Anti Conformers, and Tentative Assignments

Experimental			B3P86/6-31+G(d)		MP2/Aug-CC-pVTZ		Tentative Assignment
IR		Raman	syn-gauche	syn-anti	syn-gauche	syn-anti	
gas phase	Ar-matrix						
2012	2003 1989						2 x $\nu(C–O_b)_g$
1831	1820.0	1811	1901		1836		$\nu(C=O)_g$
1826sh	1817.8			1897		1830	$\nu(C=O)_a$
1506	1488						2 x $\nu(S–O_b)_g$
	1481						2 x $\nu(S–O_b)_a$
1463	1458.5 1457.2	1443	1443		1466		$\nu_{as}(SO_2)_g$
1458 sh	1455.8 1454.0			1429		1462	$\nu_{as}(SO_2)_a$
1223	1221.7	1213	1196		1222		$\nu_s(SO_2)_g$
1220	1220.0					1218	$\nu_s(SO_2)_a$
1220	1198.6			1196		1218	2 x $\nu(S–Cl)_a$
1201	1196.7						2 x $\nu(S–^{35}Cl)_g$
	1194.2						2 x $\nu(S–^{37}Cl)_g$
1034	1031.8 1027.8 1023.0	1033		1063		1042	$\nu(C–O_b)_a$
1016	1009.9 1002.0	1015	1057		1029		$\nu(C–O)_g$
987	985						$[\delta(SO_2) + \delta(Cl–C=O)]_g$
842	845	843	854	856	843	843	$\nu(C–Cl)_g$ / $\nu(C–Cl)_a$
753	758.0	753	713		737		$\nu(S–O)_g$
736	754.0	736		698		718	$\nu(S–O)_a$
663	666.5	660	673		675		$\delta_{oop}(C=O)_g$
	662.4			669		673	$\delta_{oop}(C=O)_a$
	601.7			582		592	$\nu(S–Cl)_a$
604	600.5	601	581		587		$\nu(S–^{35}Cl)_g$
	599.3						$\nu(S–^{37}Cl)_g$
534	536.7	535	517		525		$\delta(SO_2)_g$
	533.9			509		517	$\delta(SO_2)_a$
495		497	483		488		$\delta(Cl–C=O)_g$
		487		475		481	$\delta(Cl–C=O)_a$
		450				434	τ_a
		421	391		407		$\delta(Cl–S=O)_g$
		412				395	$\delta(Cl–S=O)_a$
		397	373		382		$\delta(Cl–S=O)_g$
		323	302		312		τ_g
		299	277		285		$\rho(SO_2)_g$
		290		272		280	$\delta(Cl–C–O)_a$
		245	229		241		$\delta(Cl–C–O)_g$
		162	145		154		$\delta(C–O–S)_o$

$$ClC(O)OSO_2Cl + TlF(s) \rightarrow ClC(O)OSO_2F + TlCl(s) \quad (7)$$

$$ClC(O)OSO_2F + TlF(s) \rightarrow ClC(O)F + TlSO_3F(s) \quad (8)$$

CONCLUSIONS

A reinvestigation of Schützenberger's classical preparation reaction for disulfuryl dichloride, $ClSO_2OSO_2Cl$, from CCl_4 and SO_3 led to the formation of a novel compound: $ClC(O)OSO_2Cl$. It is thermally stable up to 350 °C and almost photochemically stable. Upon UV−visible irradiation,

DOI: 10.1021/acs.inorgchem.8b02581
Inorg. Chem. 2018, 57, 14834−14842

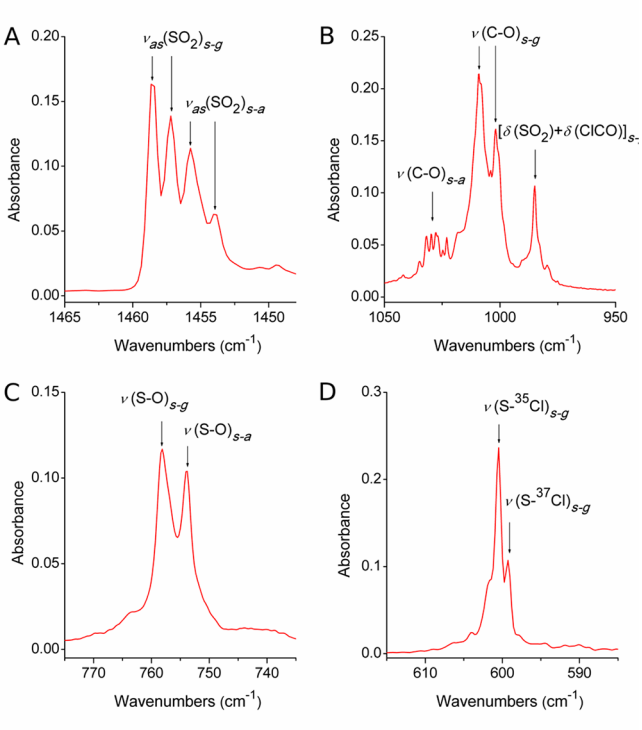

Figure 6. FTIR spectrum in the spectral region of 1465−1448 cm^{-1} (part A), 1050−950 cm^{-1} (part B), 775−735 cm^{-1} (part C), and 615−585 cm^{-1} (part D) of $ClC(O)OSO_2Cl$ isolated in an argon matrix.

only traces of the compound decompose following two different mechanisms: one giving $Cl_2C{=}O$ and SO_3 and the other Cl_2SO_2 and CO_2. $ClC(O)OSO_2Cl$ reacts violently with water, giving phosgene and sulfuric acid.

The so-far-overlooked formation of this compound from CCl_4 and SO_3 can be interpreted through a secondary reaction between one of the products, $Cl_2C{=}O$, and an excess of SO_3. We confirmed this assumption subsequently by starting from phosgene and sulfur trioxide. A high-yield one-step insertion chemical reaction gives $ClC(O)OSO_2Cl$ as the only product.

Quantum-chemical calculations predict the existence of two rotameric forms for $ClC(O)OSO_2Cl$, syn−gauche and syn−anti conformers, according to the values of ϕ(Cl−C−O−S) and ϕ(Cl−S−O−C) dihedral angles. The calculations predict the abundance of the syn−anti form to be between 22% and 15%, depending on the theoretical level of approximation. However, the existence of the syn−anti conformer could not be confirmed in a GED experiment. On the other hand, vibrational spectra (vapor-phase FTIR, liquid FT-Raman, and particularly FTIR argon-matrix spectra) were consistent with an existing equilibrium between the two conformers.

■ ASSOCIATED CONTENT

Supporting Information

The Supporting Information is available free of charge on the ACS Publications website at DOI: 10.1021/acs.inorgchem.8b02581.

Details on the quantum-chemical calculations and GED experiments, including Cartesian coordinates, structural parameters, and interatomic distances (PDF)

■ AUTHOR INFORMATION

Corresponding Authors

*E-mail: romano@quimica.unlp.edu.ar.
*E-mail: norbert.mitzel@uni-bielefeld.de.

ORCID

Rosana M. Romano: 0000-0001-5546-0504
Carlos O. Della Védova: 0000-0002-2439-2147
Xiaoqing Zeng: 0000-0003-4611-2094
Norbert W. Mitzel: 0000-0002-3271-5217

Notes

The authors declare no competing financial interest.

■ ACKNOWLEDGMENTS

R.M.R. and C.O.D.V. thank the Agencia Nacional Científica y Tecnológica ANPCyT (Grants PICT14-3266 and PICT14-2957), Facultad de Ciencias Exactas of the Universidad Nacional de La Plata (Grants UNLP-11/X684 and UNLP-11/X713), and Consejo Nacional de Investigaciones Científicas y Técnicas CONICET (Grants PIP-0352 and PIP-0348) for financial support. R.M.R. is also thankful for a DAAD fellowship. This work was financially supported by Deutsche Forschungsgemeinschaft through a core facility (GED@BI; Grant MI477/35-1).

■ REFERENCES

(1) Moreno Betancourt, A.; Schwabedissen, J.; Romano, R. M.; Della Védova, C. O.; Beckers, H.; Willner, H.; Stammler, H.-G.; Mitzel, N. W. Disulfuryl dichloride $ClSO_2OSO_2Cl$: a conformation and polymorphism chameleon. *Chem. - Eur. J.* **2018**, *24*, 10409−10421.

(2) Schützenberger, M. P. Action de l'anhydride sulfurique sur le perchlorure de carbone. *Compt. Rend.* **1869**, 352.

(3) Brauer, G. *Handbuch der Präparativen Anorganischen Chemie*; Ferdinand Enke: Stuttgart, Germany, 1975; p 389.

(4) Schnöckel, H.; Willner, H. Infrared and Raman Spectroscopy. In *Methods and Applications*; Schrader, B., Ed.; VCH: Weinheim, Germany, 1994; p 297.

(5) (a) Reuter, C. G.; Vishnevskiy, Y. V.; Blomeyer, S.; Mitzel, N. W. Gas electron diffraction of increased performance through optimization of nozzle, system design and digital control. *Z. Naturforsch., B: J. Chem. Sci.* **2016**, *71*, 1−13. (b) Berger, R. J. F.; Hoffmann, M.; Hayes, S. A.; Mitzel, N. W. An Improved Gas Electron Diffractometer − The Instrument, Data Collection, Reduction and Structure Refinement Procedures. *Z. Naturforsch., B: J. Chem. Sci.* **2009**, *64*, 1259−1268.

(6) Vishnevskiy, Y. V. The initial processing of the gas electron diffraction data: An improved method for obtaining intensity curves from diffraction patterns. *J. Mol. Struct.* **2007**, *833*, 30−41.

(7) Vishnevskiy, Y. V. The initial processing of the gas electron diffraction data: New method for simultaneous determination of the sector function and electron wavelength from gas standard data. *J. Mol. Struct.* **2007**, *871*, 24−32.

(8) Vishnevskiy, Y. V. UNEX, version 1.6.0; 2013; http://unexprog.org.

(9) (a) Sipachev, V. A. The use of quantum-mechanical third-order force constants in structural studies. *J. Mol. Struct.* **2004**, *693*, 235−240. (b) Sipachev, V. A. Local centrifugal distortions caused by internal motions of molecules. *J. Mol. Struct.* **2001**, *567−568*, 67−72. (c) Sipachev, V. A. Calculation of shrinkage corrections in harmonic approximation. *J. Mol. Struct.: THEOCHEM* **1985**, *121*, 143−151.

(10) Granovsky, A. A. Firefly, version 7.1.G; http://classic.chem.msu.su/gran/firefly/index.html.

(11) Frisch, M. J.; Trucks, G. W.; Schlegel, H. B.; Scuseria, G. E.; Robb, M. A.; Cheeseman, J. R.; Scalmani, G.; Barone, V.; Mennucci, B.; Petersson, G. A.; Nakatsuji, H.; Caricato, M.; Li, X.; Hratchian, H. P.; Izmaylov, A. F.; Bloino, J.; Zheng, G.; Sonnenberg, J. L.; Hada, M.;

DOI: 10.1021/acs.inorgchem.8b02581
Inorg. Chem. 2018, 57, 14834−14842

Ehara, M.; Toyota, K.; Fukuda, R.; Hasegawa, J.; Ishida, M.; Nakajima, T.; Honda, Y.; Kitao, O.; Nakai, H.; Vreven, T.; Montgomery, J. A., Jr.; Peralta, J. E.; Ogliaro, F.; Bearpark, M.; Heyd, J. J.; Brothers, E.; Kudin, K. N.; Staroverov, V. N.; Kobayashi, R.; Normand, J.; Raghavachari, K.; Rendell, A.; Burant, J. C.; Iyengar, S. S.; Tomasi, J.; Cossi, M.; Rega, N.; Millam, J. M.; Klene, M.; Knox, J. E.; Cross, J. B.; Bakken, V.; Adamo, C.; Jaramillo, J.; Gomperts, R.; Stratmann, R. E.; Yazyev, O.; Austin, A. J.; Cammi, R.; Pomelli, C.; Ochterski, J. W.; Martin, R. L.; Morokuma, K.; Zakrzewski, V. G.; Voth, G. A.; Salvador, P.; Dannenberg, J. J.; Dapprich, S.; Daniels, A. D.; Farkas, O.; Foresman, J. B.; Ortiz, J. V.; Cioslowski, J.; Fox, D. J. *Gaussian 09*, revision D.01; Gaussian, Inc.: Wallingford, CT, 2009.

(12) Gledding, E. D.; Badenhoop, J. K.; Reed, A. E.; Carpenter, J. E.; Bohmann, J. A.; Morales, C. M.; Landis, C. R.; Weinhold, F. *NBO 6.0*; Theoretical Chemistry Institute, University of Wisconsin: Madison, WI, 2013; http://nbo6.chem.wisc.edu.

(13) Keith, T. A. AIMALL, version 16.05.18; TK Gristmill Software: Overland Parks, KS, 2016; http://aim.tkgristmill.com.

(14) (a) Dunning, T. H. Gaussian basis sets for use in correlated molecular calculations. I. The atoms boron through neon and hydrogen. *J. Chem. Phys.* **1989**, *90*, 1007. (b) Handy, N. C.; Cohen, A. J. Left-right correlation energy. *Mol. Phys.* **2001**, *99*, 403−412.

(15) (a) Lee, C.; Yang, W.; Parr, R. G. Development of the Colle-Salvetti correlation-energy formula into a functional of the electron density. *Phys. Rev. B: Condens. Matter Mater. Phys.* **1988**, *37*, 785−789. (b) Becke, A. D. Density-functional exchange-energy approximation with correct asymptotic behavior. *Phys. Rev. A: At., Mol., Opt. Phys.* **1988**, *38*, 3098−3100.

(16) Goerigk, L.; Grimme, S. Efficient and accurate Double-Hybrid-Meta-GGA density functionals—evaluation with the extended GMTKN30 database for general main group thermochemistry, kinetics, and noncovalent interactions. *J. Chem. Theory Comput.* **2011**, *7*, 291−309.

(17) Møller, C.; Plesset, M. S. Note on an Approximation Treatment for Many-Electron Systems. *Phys. Rev.* **1934**, *46*, 618−622.

(18) Erben, M. F.; Della Védova, C. O.; Boese, R.; Willner, H.; Oberhammer, H. Trifluoromethyl chloroformate, $ClC(O)OCF_3$: structure, conformation, and vibrational analysis studied by experimental and theoretical methods. *J. Phys. Chem. A* **2004**, *108*, 699−706.

(19) Arce, V. B.; Della Védova, C. O.; Downs, A. J.; Parsons, S.; Romano, R. M. Trichloromethyl chloroformate ("diphosgene"), $ClC(O)OCCl_3$: structure and conformational properties in the gaseous and condensed phases. *J. Org. Chem.* **2006**, *71*, 3423−3428.

(20) Della Védova, C. O.; Downs, A. J.; Moschione, E.; Parsons, S.; Romano, R. M. Chlorocarbonyl trifluoromethanesulfonate, $ClC(O)-OSO_2CF_3$: structure and conformational properties in the gaseous and condensed phases. *Inorg. Chem.* **2004**, *43*, 8143−8149.

(21) Trautner, F.; Della Védova, C. O.; Romano, R. M.; Oberhammer, H. Gas Phase structure and conformational properties of chlorocarbonyl trifluoromethanesulfonate, $ClC(O)OSO_2CF_3$. *J. Mol. Struct.* **2006**, *784*, 272−275.

(22) Della Védova, C. O.; Downs, A. J.; Novikov, V. P.; Oberhammer, H.; Parsons, S.; Romano, R. M.; Zawadski, A. Fluorocarbonyl Trifluoromethanesulfonate, $FC(O)OSO_2CF_3$: structure and conformational properties in the gaseous and condensed phases. *Inorg. Chem.* **2004**, *43*, 4064−4071.

(23) (a) Kohn, W.; Sham, L. J. Self-consistent equations including exchange and correlation effects. *Phys. Rev.* **1965**, *140*, A1133−A1138. (b) Hohenberg, P.; Kohn, W. Inhomogeneous Electron Gas. *Phys. Rev.* **1964**, *136*, B864−B871.

(24) Gil, D. M.; Tuttolomondo, M. E.; Blomeyer, S.; Reuter, C. G.; Mitzel, N. W.; Altabef, A. B. Gas-phase structure of 2,2,2-trichloroethyl chloroformate studied by electron diffraction and quantum-chemical calculations. *Phys. Chem. Chem. Phys.* **2016**, *18*, 393−402.

(25) Durig, J. R.; Griffin, M. G. The microwave, Raman, far infrared, and NMR spectra and structure of methylchloroformate. *J. Mol. Spectrosc.* **1977**, *64*, 252−266.

(26) Hargittai, I.; Schultz, G.; Kolonits, M. Electron-diffraction investigation of the molecular structure of methyl chlorosulphate. *J. Chem. Soc., Dalton Trans.* **1977**, 1299−1302.

(27) Tuttolomondo, M. E.; Argañaraz, P. E.; Varetti, E. L.; Hayes, S. A.; Wann, D. A.; Robertson, H. E.; Rankin, D. W.; Ben Altabef, A. Gas-phase structure and vibrational properties of trifluoromethyl trifluoromethanesulfonate, $CF_3SO_2OCF_3$. *Eur. J. Inorg. Chem.* **2007**, *2007*, 1381−1389.

(28) (a) Reed, A. E.; Curtiss, L. A.; Weinhold, F. Intermolecular interactions from a natural bond orbital, donor-acceptor viewpoint. *Chem. Rev.* **1988**, *88*, 899−926. (b) Weinhold, F. Natural bond orbital analysis: A critical overview of relationships to alternative bonding perspectives. *J. Comput. Chem.* **2012**, *33*, 2363−2379.

(29) (a) Badenhoop, J. K.; Weinhold, F. Natural steric analysis of internal rotation barriers. *Int. J. Quantum Chem.* **1999**, *72*, 269−280. (b) Badenhoop, J. K.; Weinhold, F. Natural steric analysis: Ab initio van der Waals radii of atoms and ions. *J. Chem. Phys.* **1997**, *107*, 5422−5432. (c) Badenhoop, J. K.; Weinhold, F. Natural bond orbital analysis of steric interactions. *J. Chem. Phys.* **1997**, *107*, 5406−5421.

(30) (a) Bader, R. F. W. A quantum theory of molecular structure and its applications. *Chem. Rev.* **1991**, *91*, 893−928. (b) Bader, R. F. W. *Atoms in Molecules. A Quantum Theory*; Clarendon Press: Oxford, U.K., 2003.

(31) Kagarise, R. E. Relation between the electronegativities of adyacent susbtituents and the stretching frequencies of the carbonyl group. *J. Am. Chem. Soc.* **1955**, *77*, 1377−1379.

(32) Bohets, H.; van der Veken, B. J. Raman and infrared spectra, conformational stability, vibrational assignment and ab initio calculations for ethyl chloroformate. *J. Raman Spectrosc.* **1995**, *26*, 821−834.

(33) Tobón, Y. A.; Di Loreto, H. E.; Della Védova, C. O.; Romano, R. M. Matrix isolation study of ethyl chloroformate, $ClC(O)-OCH_2CH_3$. *J. Mol. Struct.* **2008**, *881*, 139−145.

(34) Romano, R. M.; Della Védova, C. O.; Beckers, H.; Willner, H. Photochemistry of $SO_2/Cl_2/O_2$ gas mixtures: Synthesis of the new peroxide $ClSO_2OOSO_2Cl$. *Inorg. Chem.* **2009**, *48*, 1906−1910.

(35) Chaabouni, H.; Schriver-Mazzuoli, L.; Schriver, A. Conversion of SO_2 to SO_3 by in situ photolysis of SO_2 and O_3 mixtures isolated in argon matrixes: isotopic effects. *J. Phys. Chem. A* **2000**, *104*, 3498−3507.

(36) Mincu, I.; Allouche, A.; Cossu, M.; Aycard, J.-P.; Pourcin, J. FT-IR identification, characterization and ab initio vibrational analysis of phosgene, oxalyl chloride and 1,2-dichlorocyclobutene-3,4-dione trapped in argon cryogenic matrices. *Spectrochim. Acta, Part A* **1995**, *51*, 349−362.

(37) Bahou, M.; Chen, S.-F.; Lee, Y.-P. Production and infrared absorption spectrum of $ClSO_2$ in matrices. *J. Phys. Chem. A* **2000**, *104*, 3613−3619.

DOI: 10.1021/acs.inorgchem.8b02581
Inorg. Chem. 2018, 57, 14834−14842